Laboratory and In Situ Observation of Deposition Growth of Frozen Drops

ALEXEI V. KOROLEV

Sky Tech Research, Inc., Richmond Hill, Ontario, Canada

MATTHEW P. BAILEY AND JOHN HALLETT

Desert Research Institute, Reno, Nevada

GEORGE A. ISAAC

Cloud Physics Research Division, Meteorological Service of Canada, Toronto, Ontario, Canada

(Manuscript received 18 March 2003, in final form 10 November 2003)

ABSTRACT

The water vapor deposition growth of frozen drops with diameter greater than 100 μm has been studied in a thermal diffusion chamber. For varying periods of time, it was found that frozen drops experience spherical growth. The characteristic time of spherical growth depends on supersaturation, temperature, and drop size, and it varies from minutes to tens of minutes. The average rate of frozen drop growth agrees well with that predicted by the Maxwellian growth equation for ice spheres. Observations in natural clouds conducted with a cloud particle imager probe has yielded evidence that frozen drops may retain spheroidal shapes for at least 15–20 min under conditions close to saturation over water. These observations are in agreement with the laboratory experiments. The observation of frozen drops in natural clouds may be correlated to freezing drizzle generated by overlying cloud layers that may lead to hazardous in-flight icing.

1. Introduction

Under conditions typical for the troposphere, water vapor crystallizes with a sixfold symmetry and forms simple hexagonal crystals with two basal planes and six prism planes in addition to polycrystalline forms of varying complexity. Laboratory experiments revealed that the rate of propagation of the basal faces relative to that of prism faces varies with temperature and supersaturation in a characteristic manner (e.g., Nakaya 1954; Kobayashi 1957; Hallett and Mason 1958). Observations summarized by Magono and Lee (1966) showed a variety of hexagonal structures in ice particles grown in natural clouds. The diffusional growth of ice crystals can be treated in the same manner as for drops by making an analogy between the governing equation and boundary conditions for electrostatic and diffusional problems (Jeffreys 1918; Houghton 1950). The diffusional growth equation can be formally applied to ice spheres. This approach has been used in a number of numerical models for estimations of the rate of growth of ice crystals in clouds. However, the spherical growth of ice particles has been considered as a hypothetical possibility that does not exist in nature. Laboratory experiments (Yamashita and Takahashi 1972; Magono et al. 1976; Gonda and Yamazaki 1984) showed that small droplets with diameter $D < 20$ μm, after freezing, initially grow as polyhedra with 20 facets. The pyramidal faces then rapidly disappear and the ice particle exhibits columnar or plate growth depending on supersaturation and temperature. Observations of large drops ($D > 100$ μm) frozen in natural cloud or under laboratory conditions indicate that nucleation and initial growth occur differently in comparison with small droplets. In specific terms, no pyramidal faces form on large frozen drops. Laboratory experiments revealed that bulges, protrusions, or spikes may form on the surface of large drops during freezing (e.g., Puzanov and Akkuratov 1952; Johnson and Hallett 1968; Takahashi 1975; Wood et al. 2002). This result is in agreement with microphotographs of ice pellets, sleet, and grains collected on the ground (e.g., Bentley 1907; Bergeron 1938; Kimura and Kajikawa 1984). Laboratory studies also showed that drops, depending on size, temperature, and ventilation, may shatter during freezing (e.g., Puzanov and Akkuratov 1952; Johnson and Hallett 1968; Takahashi 1975, 1976).

This paper describes laboratory experiments on the

Corresponding author address: Alexei V. Korolev, Sky Tech Research, Inc., 28 Don Head Village Blvd., Richmond Hill, ON L4C 7M6, Canada.
E-mail: alexei.korolev@rogers.com

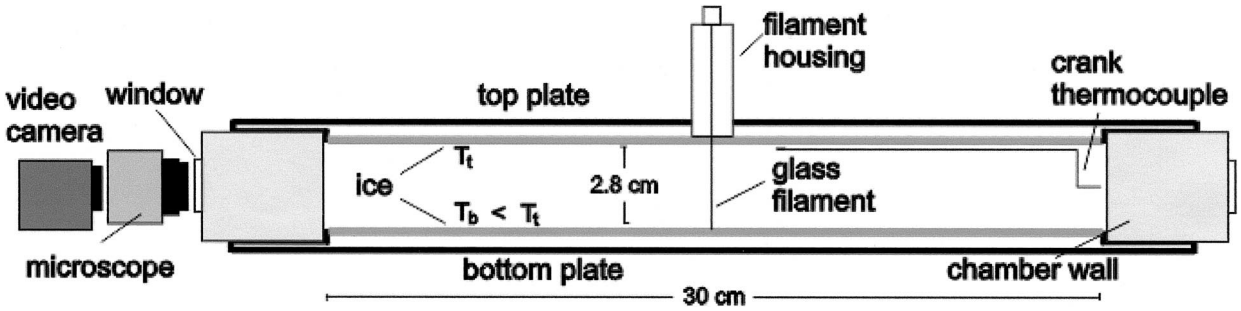

FIG. 1. Schematic of the static diffusion chamber used in the study.

diffusional growth of ice spheres from vapor with $D > 100$ μm. The results of the experiment are compared with the observations of frozen drops in natural clouds. The study was focused on the following questions: How does the shape of frozen spheres change with time? How long can it be recognized as a sphere before it changes shape appreciably? Can the Maxwell equation of the diffusional growth of spheres be applied to frozen drops?

2. Experimental installation

The thermal diffusion chamber (Fig. 1) used in this study has been developed in the Ice Physics Laboratory of the Desert Research Institute for the growth of ice crystals from the vapor at known temperature and supersaturation. A schematic of the thermal diffusion chamber is shown in Fig. 1.

The chamber consists of two stainless steel plates separated by a short, thick, acrylic cylinder. The top plate has a stainless steel wick, which can be saturated with water, and the bottom plate is covered by a 3-mm-thick layer of water. The proportion between the diameter of the plates (30 cm) and the distance between them (2.8 cm) provides uniform (in radial direction) profiles of temperature and supersaturation in the central part of the chamber and reduces the effect of walls (e.g., Elliott 1971). The temperatures of the two plates are independently controlled by refrigeration units, and, once the liquid layers are frozen, a difference in temperature between the two creates an environment supersaturated with respect to ice. Two double-paned windows set in recessed ports in the chamber wall allow illumination and observation. Illumination was cooled with a long column of water and two infrared filters leading to a temperature increase undetectable by a thermocouple with a sensitivity of 0.1°C. A small flow of dry air between the panes keeps them ice free so that crystal growth can be observed and recorded with a time-lapse camera and microscope system.

To study frozen drop growth, ice crystals were initially nucleated and grown on 50-μm glass filaments suspended in the center of the chamber at the temperature to be studied, with the plate temperatures set to give highly supersaturated conditions. Crystals were rapidly grown to various sizes and then were completely melted with a stream of dry nitrogen introduced via a small stainless steel tube from a port in the side of the chamber. This step was done after the ice supersaturation had been reduced to zero, or a nominally low value, by making the two plates isothermal. This process allowed drops to be formed of a predetermined size by evaporating most of the smaller drops left adhering to the filament. Once the desired drop sizes were obtained, they were nucleated by briefly introducing a copper rod into the chamber that had been cooled with liquid nitrogen, freezing the drops by touching the glass filament, or by contact nucleation from small crystals nucleated by the cold rod in a slightly supersaturated chamber environment. Drops of a few hundred micrometers in diameter froze solid and reached environmental conditions in less than 1 min. Once the drops had reached equilibrium, the temperatures of the two plates were changed to create a desired supersaturation, and the growth was recorded. The glass filament could be rotated so that frozen drops could be viewed from any angle as growth proceeded. The study was carried out at a laboratory air pressure of 850 hPa.

3. Laboratory observation of frozen drop depositional growth

A set of 10 experiments of frozen drop depositional growth was conducted for different temperatures from $-4°$ to $-20°$C and supersaturation over ice S_i from 0.02 to 0.21. The sequences of successive images of growing ice particles are shown in Figs. 2–5. To analyze the growth rate of ice spheres, the contour of the ice particle image at the moment of complete freezing was superimposed with those for later times (Figs. 2d,e; 3d,e; 4e,f,g; 5f,g,h). This technique enables accurate evaluation of the changes with time in size, mass, and shape of the ice particle. Because of capillary forces, the drops attached to a glass filament appear as prolate spheroids. In the following discussion, the dimensions of such drops will be characterized by $D_{\min}$ and $D_{\max}$, that is, sizes perpendicular and parallel to the filament, respectively. A brief description of 4 of the 10 experiments is given below.

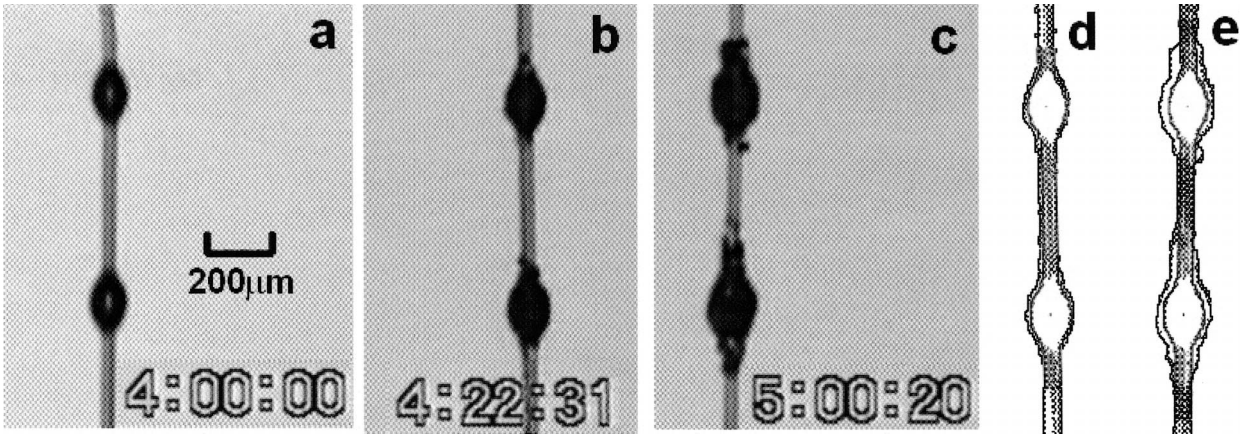

FIG. 2. (a)–(c) Sequence of images of frozen drops growing in a thermal diffusion chamber at $T = -14$°C and $S_i = 0.02$; (d) superposition of contours of images (a) and (b); (e) contours of images (a) and (c). Numbers at the bottom of diagrams (a)–(c) indicate time in hours, minutes, and seconds.

a. $S_i = 0.02$, $T = -14$°C

Figures 2a–c show a sequence of images of ice particles growing on a filament at supersaturation over ice $S_i = 0.02$ and temperature $T = -14$°C. The characteristic size of the frozen drops in the direction perpendicular to the filament at the moment of nucleation was about $D_{\min} = 125$ μm. In 1 h, the size of the ice particles increased to $D_{\min} = 165$ μm. Figures 2d and 2e show that within 1 h the frozen drops were growing approximately uniformly layer by layer.

b. $S_i = 0.06$, $T = -14$°C

Figures 3a–c show images of ice particles growing at a temperature of $T = -14$°C and a supersaturation over ice of $S_i = 0.06$. This corresponds to approximately one-half water saturation at this temperature. The initial size of the top drop at the moment of freezing was $D_{\min} = 220$ μm (Fig. 3a). Figures 3a–c show spherical growth of ice spheres as in the previous case but at higher supersaturation. However, after about 0.5 h, individual ice crystals start to grow out of the surface of the top frozen drop, as seen in Figs. 3b and 3c.

c. $S_i = 0.08$, $T = -7.5$°C

The growth of frozen drops was conducted at $T = -7.5$°C at an ice supersaturation near water saturation, which corresponds to approximately $S_i = 0.08$. Figure 4 shows the sequence of ice particle growth during the 33 min after the moment of drop freezing. During the first 10 min, the surface of the frozen drop stays relatively smooth (Fig. 4b). After 33 min, at 1630 LT, the roughness of the surface increases and some small columns or thick plates extend from the surface of the frozen drop (Fig. 4d). Nevertheless after 0.5 h of growth near water saturation, the spherical shape of the growing ice particle is clearly recognizable.

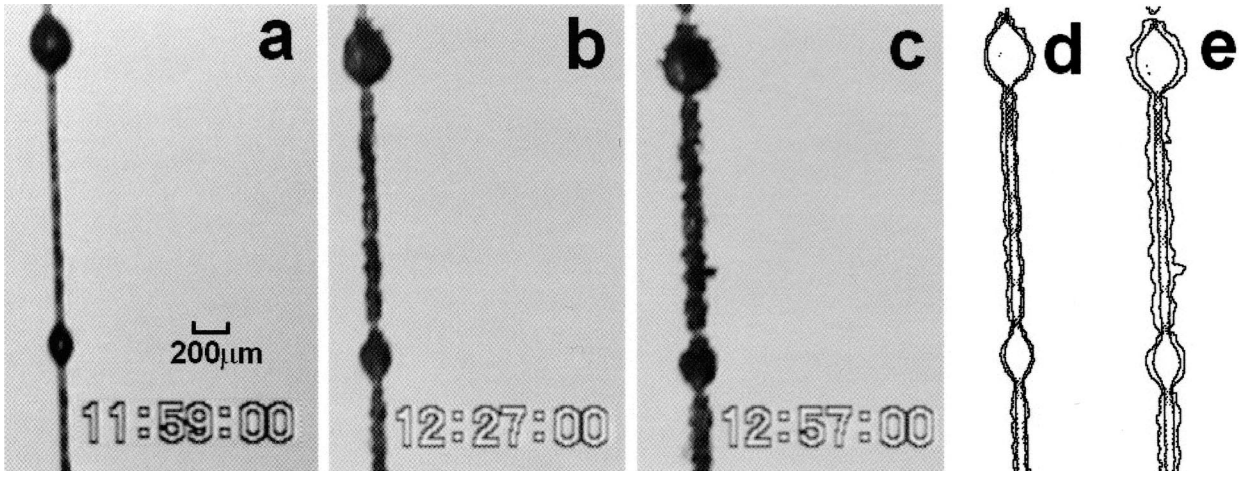

FIG. 3. Same as in Fig. 2 but for $T = -14$°C and $S_i = 0.06$.

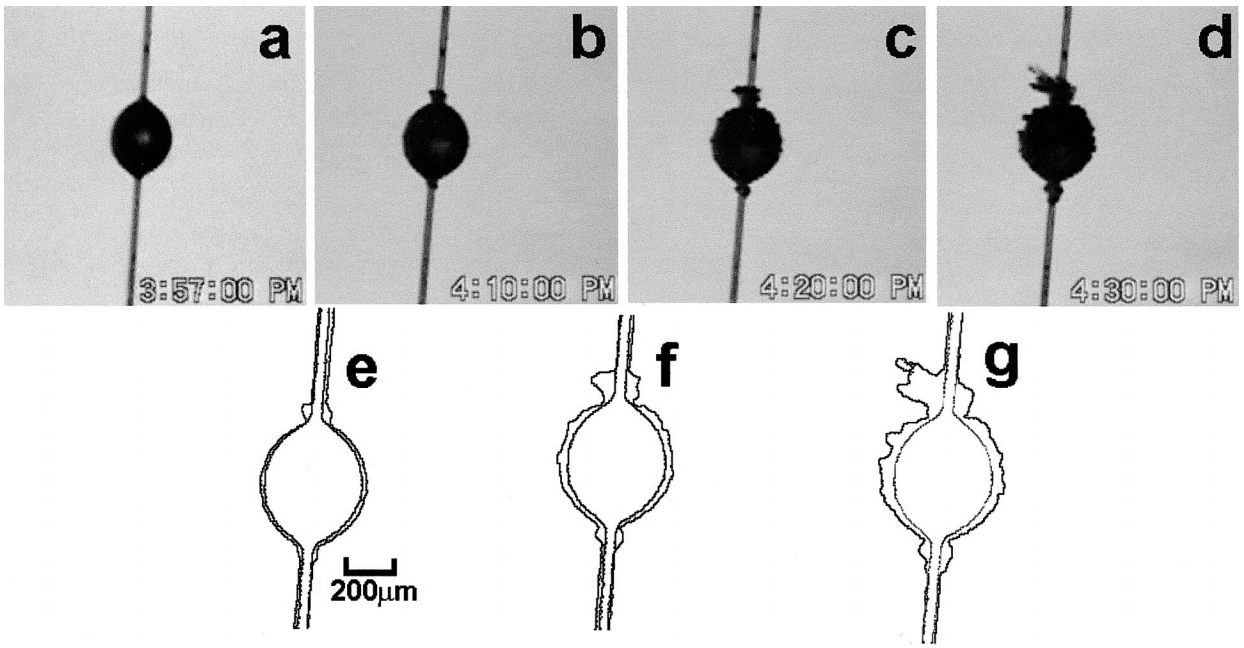

FIG. 4. (a)–(d) Same as in Fig. 2 for $T = -7.5$°C and $S_i = 0.08$; (e) superposition of contours of images (a) and (b); (f) contours of images (a) and (c); (g) contours of images (a) and (d). Numbers at the bottom of diagrams (a)–(d) indicate time in hours, minutes, and seconds.

d. $S_i = 0.14$, $T = -12$°C

In this experiment, a drop of approximately 800 μm in diameter was placed at the end of the filament. The drop was nucleated and frozen under low supersaturation, which was slowly increased thereafter (Figs. 5a,b). At approximately 1223 LT (Fig. 5c), the ice supersaturation exceeded water saturation, that is, about 0.14 supersaturation over ice. After that moment, S_i stayed approximately constant and the ice particles were grown under constant conditions. While the ice supersaturation increased toward water saturation, quasi-spherical growth of the frozen drop was observed (Figs. 5f,g) and ice spears started to grow out of the frozen drop. During the approximately 15 min from 1223 to 1238 near water saturation, the frozen drop was completely covered by ice crystals growing in radial directions, which made the spherical shape of the ''source'' particle difficult to recognize.

4. Comparison with Maxwellian growth

The rate of mass growth of ice particles in the thermal diffusion chamber was estimated from the contour images of the frozen drops. The volume of the particles was calculated by assuming that the drops were prolate spheroids (hereinafter referred to simply as spheroids). The small and large axes of the spheroids were derived from the contour diagrams (e.g., Figs. 2d,e; 3d,e; 4e,f,g). Rotation of the glass filament and the supported particles through 360° showed that the frozen drops were generally uniform until the point at which substantial extended surface features developed. This result provided a basis to assume that the density of ice-grown spheres was approximately 900 kg m^{-3}. The ice particles growing out of the frozen drops at the late stage of growth were not included in the mass calculations, and incremental mass calculations were terminated when the development of extended surface features became substantial.

The estimated mass growth of the particles was compared with that calculated from the equation of diffusion ice growth,

$$dM/dt = 4\pi CBS_i. \tag{1}$$

Here, S_i is the supersaturation over ice,

$$B = \frac{1}{\dfrac{R_v T}{E_i D} + \dfrac{L_i}{KT}\left(\dfrac{L_i}{R_v T} - 1\right)}$$

(e.g., Pruppacher and Klett 1997; Hallett et al. 2002), E_i is the saturation of the water vapor over ice at temperature T, D is the coefficient of water vapor diffusion, R_v is the gas constant for water vapor, K is the coefficient of air heat conductivity, L_i is latent heat of fusion, and C is the capacitance, which is a function of particle geometry. Thermal accomodation and deposition coefficients in Eq. (1) are assumed to be equal to 1. For a prolate spheroid with semimajor and minor axes $a = D_{\max}/2$ and $b = D_{\min}/2$,

$$C = \frac{A}{\ln[(a + A)/b]}, \quad \text{with } A = \sqrt{a^2 - b^2}. \tag{2}$$

Figure 6 shows comparisons of the mass growth in-

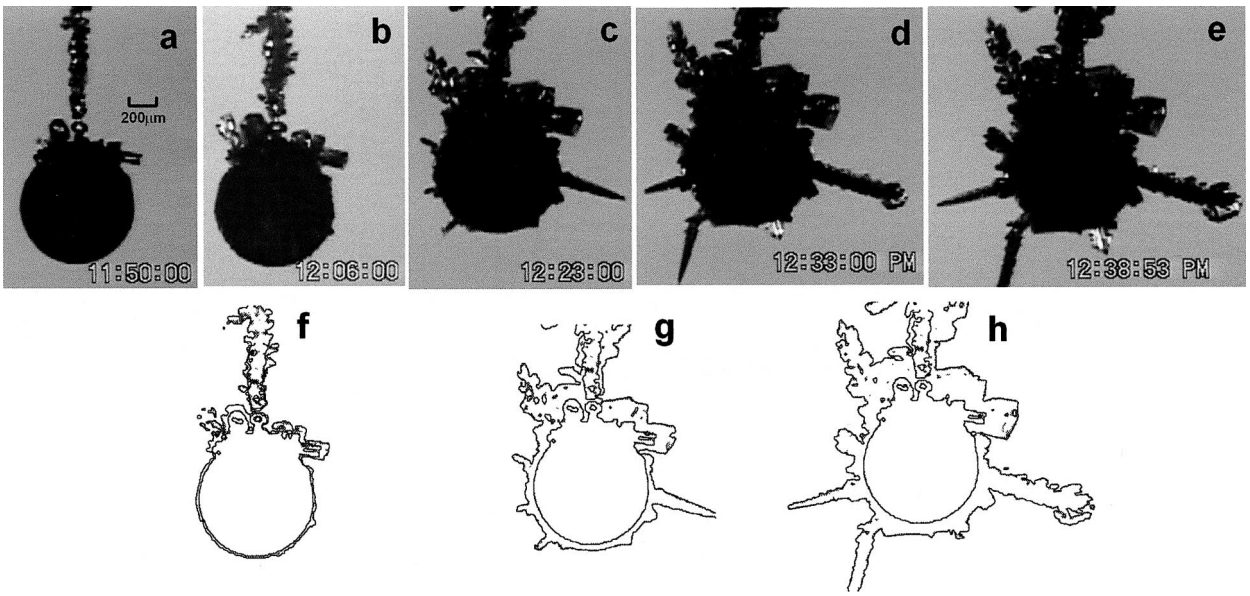

FIG. 5. Same as in Fig. 2 but for (a), (b) $T = -12$°C and $S_{i0} < S_i < S_{w0}$ and (c)–(e) $T = -12$°C and $S_i = 0.14$; (f) superposition of contours of images (a) and (b); (g) contours of images (a) and (c); (h) contours of images (a) and (d).

crement measured experimentally (ΔM_{exp}) and that calculated from Eq. (1) (ΔM_{theor}), where it can be seen that the ice particle mass estimated for the case of spherical growth agrees well with that observed during growth in the thermal diffusion chamber. However, for some cases, the difference between the theoretical and experimental values may reach 20%–30%. These differences or potential errors are related to the determination of supersaturation from temperature measurements (top and bottom temperatures drifted slightly at the warmest temperatures studied) and the measurements of frozen drop sizes. The accuracy of the measurement of particle sizes from the images was about two pixels, which corresponds to approximately 10–20 μm. For a 100-μm-diameter drop, this accuracy would correspond to approximately 10% error in size and 30% error in mass. For larger drops the relative error of the estimation of drop mass is smaller. The error in supersaturation did not exceed 5% and usually was approximately 1% of the estimated value of S_i.

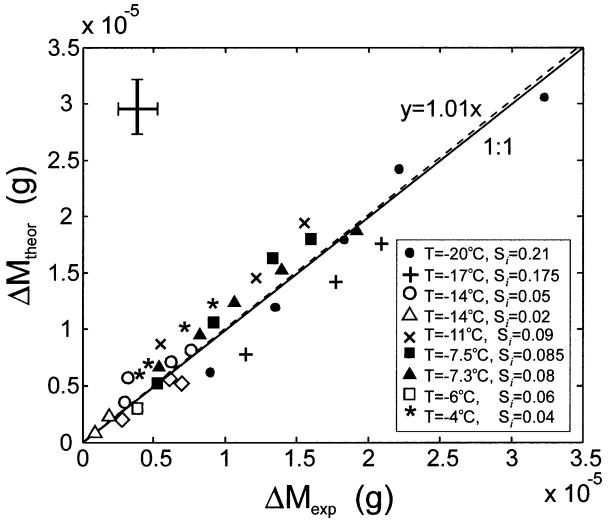

FIG. 6. Comparison of the incremental mass growth calculated from Eq. (1) with that derived from experimental data. Frozen drops were grown in still air with no ventilation. The initial size of the frozen drops ranged from 100 to 800 μm, and the origin represents the initial incremental mass at the time of freezing. The cross in the upper-left corner indicates the error bars.

5. In situ observation of frozen drops in natural clouds

The objective of this section is to demonstrate that frozen drops formed in natural clouds may retain a spherical shape during a characteristic time of approximately 20 min under relative humidity conditions close to saturation over water. It is difficult in the laboratory to reproduce the varying conditions of temperature and supersaturation along the pathway of each individual frozen drop falling through clouds; however, the in situ observations of frozen drops qualitatively support the laboratory observations previously described.

The in situ observation of frozen drops was conducted with the cloud particle imager (CPI) (Lawson et al. 2001) installed on the National Research Council Convair 580. The CPI provides the images of cloud particles with 256 gray levels and a 2.3-μm pixel resolution. The images of ice particles shown below were collected on 17 February 1999 in a deep altostratus–nimbostratus (As–Ns) cloud system in an approaching front over the northern part of Lake Ontario during the Canadian

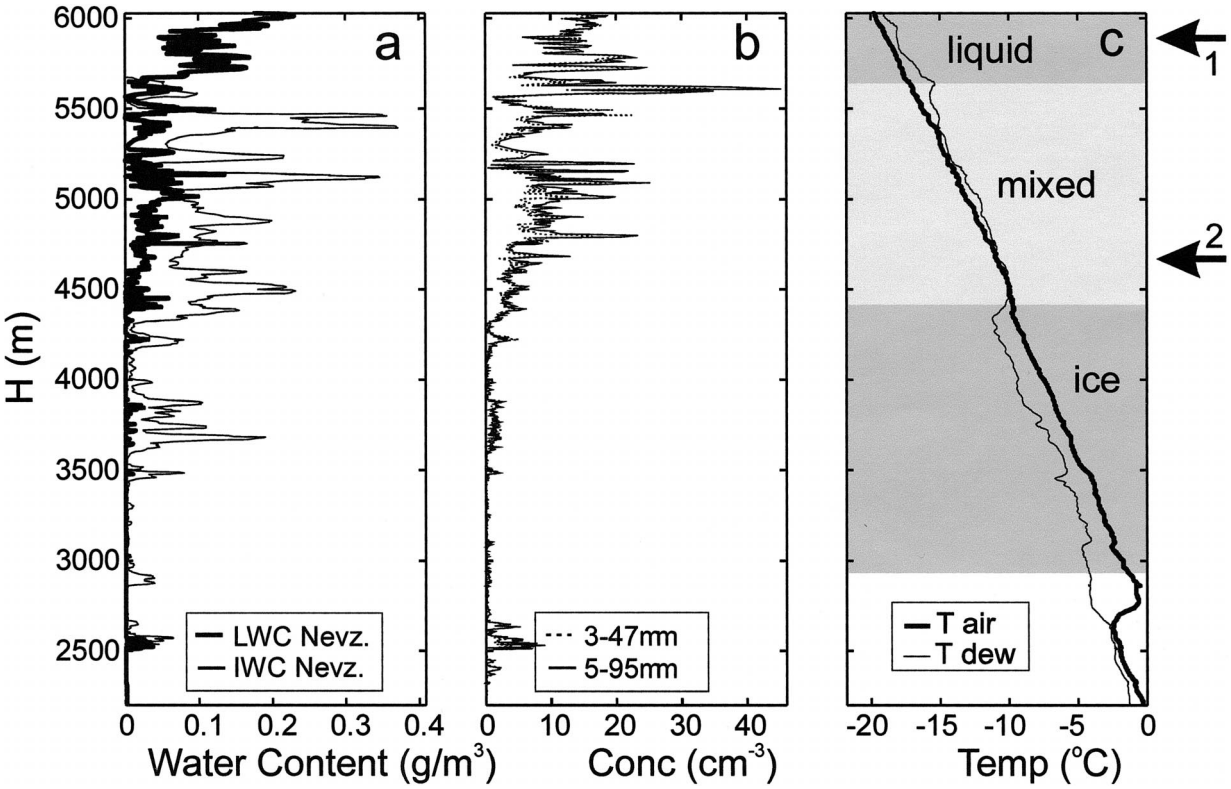

FIG. 7. Vertical profiles of (a) liquid and ice water content measured by a Nevzorov probe, (b) concentration of cloud particles measured by two FSSPs in the ranges 3–47 and 5–95 μm, and (c) air temperature measured by the Rosemount temperature probe and dewpoint temperature measured by EG&G hygrometer. Measurements were conducted in As–Ns at 1757:18–1816:56 UTC 17 Feb 1998 over the northern part of Lake Ontario.

Freezing Drizzle Experiment 3 (CFDE3; Isaac et al. 2001). The flight was arranged as five spiral ascents and descents between 2000 and 6200 m over two different spots located about 35 km apart. Though each vertical sounding resulted in different profiles of microphysical parameters, all five profiles clearly indicate a sustained liquid layer near cloud top (approximately between 5600/5200 and 6200 m), a mixed-phase layer in the middle part (between 4400/3800 and 5600/5200 m), and a glaciated bottom part (below 4400/3800 m). The drizzle-sized drops were observed through the whole upper layer. The diagrams presented in Fig. 7 show one of five vertical profiles of ice and liquid water content measured by the Nevzorov probe (Korolev et al. 1998), the concentration of cloud particles measured by a forward-scattering spectrometer probe (FSSP; Knollenberg 1981), and air and dewpoint temperature, measured by the Rosemount, Inc., reverse-flow probe and EG&G, Inc., hygrometer. The Nevzorov probe data (Fig. 7a) indicate that the layer near cloud top from 5600 to 6100 m was liquid, the layer from 4400 to 5600 m was mixed, and the layer from 2900 to 4400 m was completely glaciated.

Figure 8 shows images of cloud particles measured by the CPI at two different levels indicated by the arrows (1 and 2) on the right of Fig. 7. The top panel of Fig. 8 shows images of drizzle-sized drops of 100–200 μm in diameter generated by the top cloud layer. The terminal fall velocity of such drops at this altitude is about 0.4–1 m s^{-1}. The bottom panel of Fig. 8 shows the images of cloud particles taken approximately 1300 m below the images shown in the top panel. At least 10 particles in the bottom panel of Fig. 8 may be identified as frozen drops. Some of the frozen drops accreted to bigger ice particles may have frozen prior to or following the accretion.

The air in the mixed cloud layer (4400–5600 m) caused by the presence of liquid droplets was close to saturation over water. The frozen drops in the bottom panel of Fig. 8 retained spherical or quasi-spherical shapes and none of them had developed any significant ice crystal structures on their surface under conditions close to saturation over water. It is not clear when the drops froze and how long they were subjected to the depositional growth as ice particles after the moment of freezing. However, the maximum time of the depositional growth can be estimated as 15–20 min, the time required for them to fall out of the liquid layer (5500 m; Fig. 7c) and reach the level associated with the bottom panel of Fig. 8 (4600 m) at a fall velocity of 0.7–1 m s^{-1}.

Figures 9 and 10 show the CPI images of frozen drops

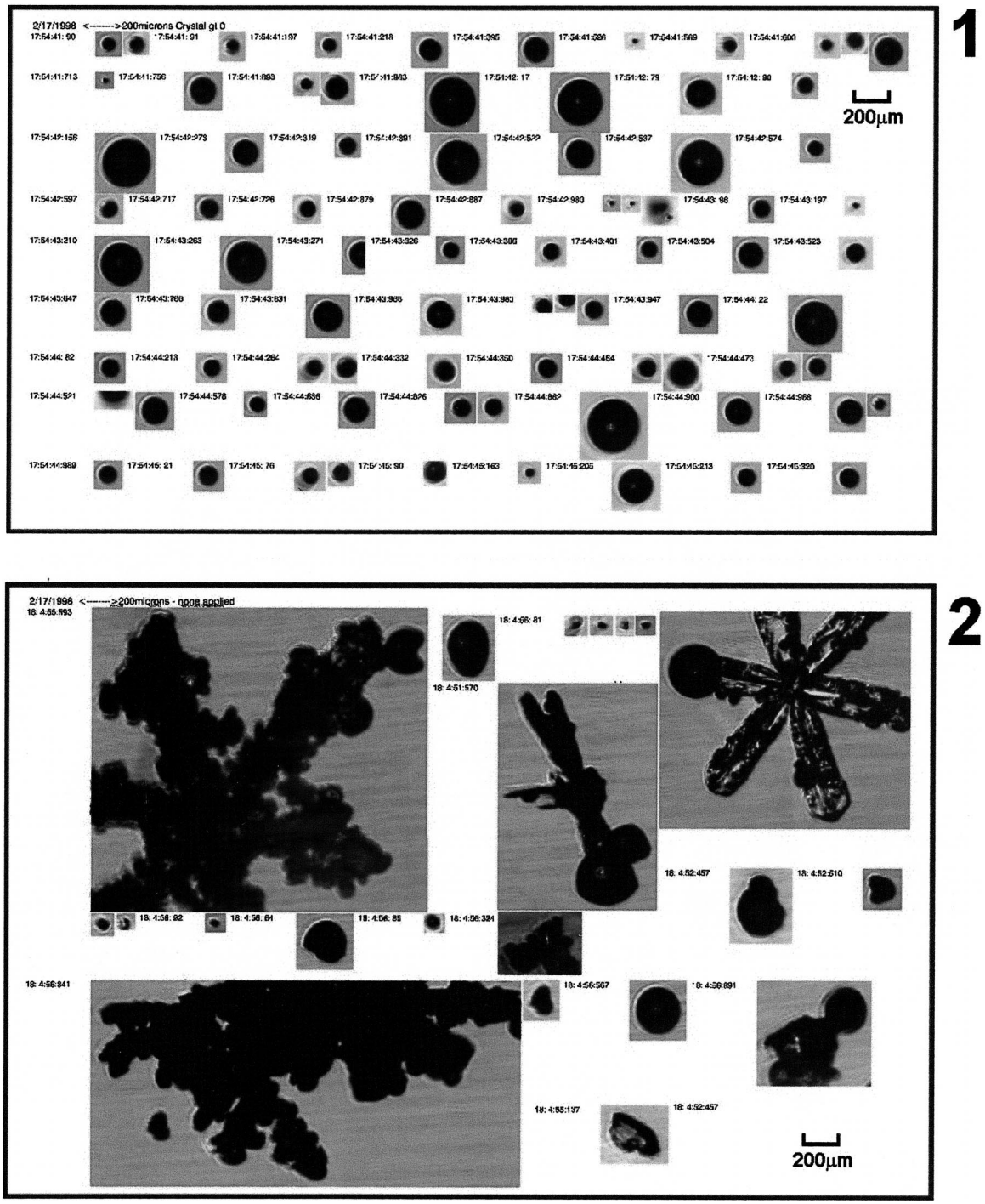

FIG. 8. Images of cloud particles measured by CPI at two different levels indicated by arrows (top) ''1'' and (bottom) ''2,'' respectively, on the right in Fig. 7.

collected in a mixed-phase cloud layer between 4400 and 5600 m (Fig. 7). The shape of the drops during freezing has changed because of the formation of bulges, protrusions, and spikes on their surfaces (Fig. 9a). Such changes in the shape of drops during freezing were observed in laboratory experiments (e.g., Johnson and Hallett 1968; Takahashi 1975; Uyeda and Kikuchi 1978).

Figure 9b shows chunks of frozen drops, which could result from shattering during freezing. Similar patterns of shattered large drops were also observed in laboratory

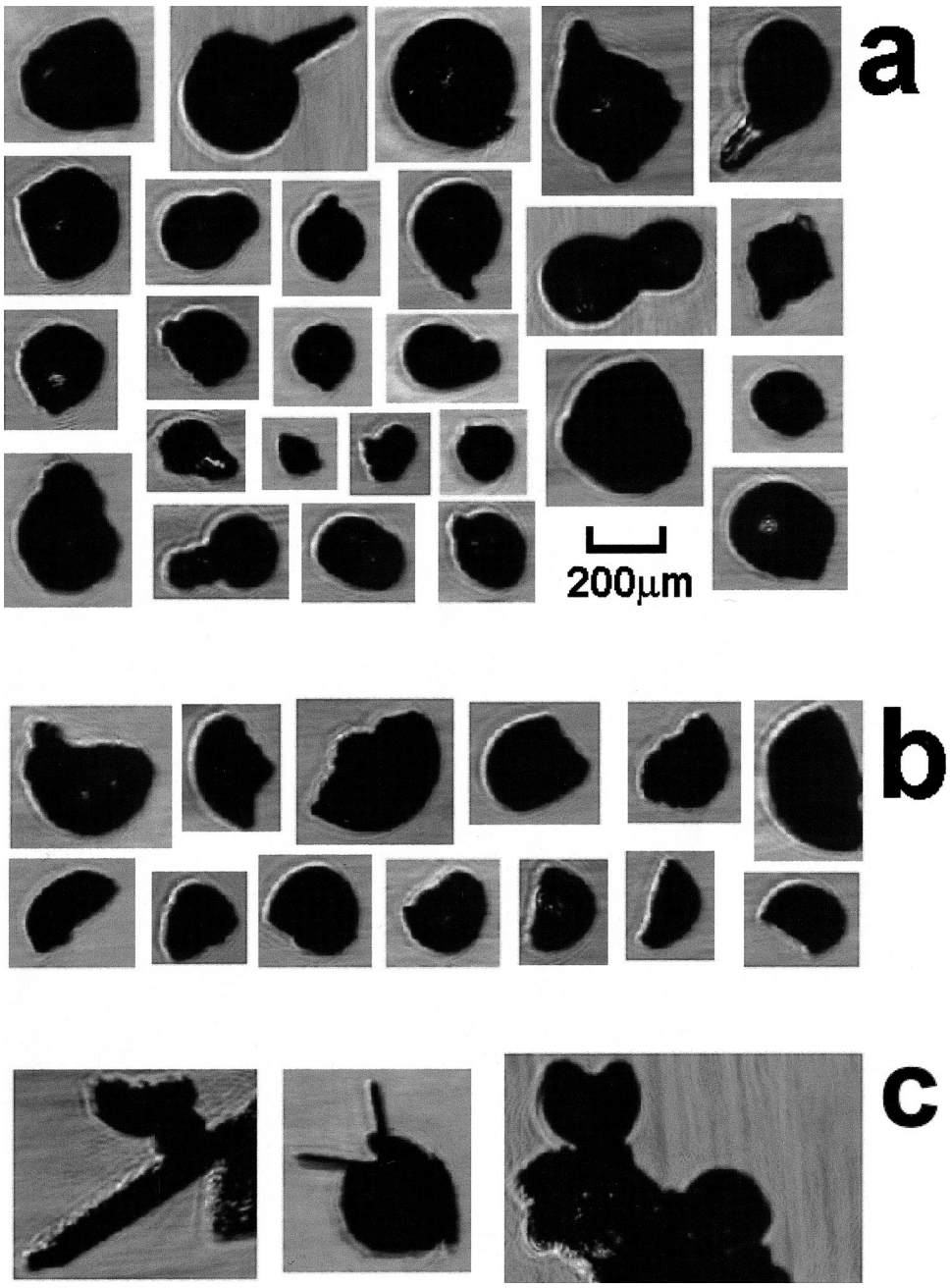

FIG. 9. Images of frozen drops detected by a CPI during a sounding between 4400 and 5600 m (Fig. 7) in a mixed-phase cloud layer: (a) frozen drops with bulges, protrusions, and spikes; (b) single shattered frozen drops; and (c) shattered frozen drops attached to ice particles.

experiments by Johnson and Hallett (1968) and Takahashi (1975, 1976). The shattered drops were additionally observed at temperatures colder than those relevant to the Hallett–Mossop process for droplet shattering ($-2° > T_{HM} > -8°C$). The images of shattered drops adhering to bigger ice particles in the left and right image of Fig. 9c show drops shattered by freezing on accretion, influenced by heat flow into the colder ice base. The center image of ice crystals growing out of the crack clearly demonstrates the occurrence of vapor grown crystals on a previously frozen and shattered freely falling drop. This image is the only example found in this dataset, suggesting that such events are rare. The images in Fig. 9c suggest that the shattering effect is genuine, rather than an artifact resulting from impact with the sampling inlet tube of the CPI probe. Calculations of the kinetic energy of drops impacting the solid surface at typical aircraft speeds indicate that such a

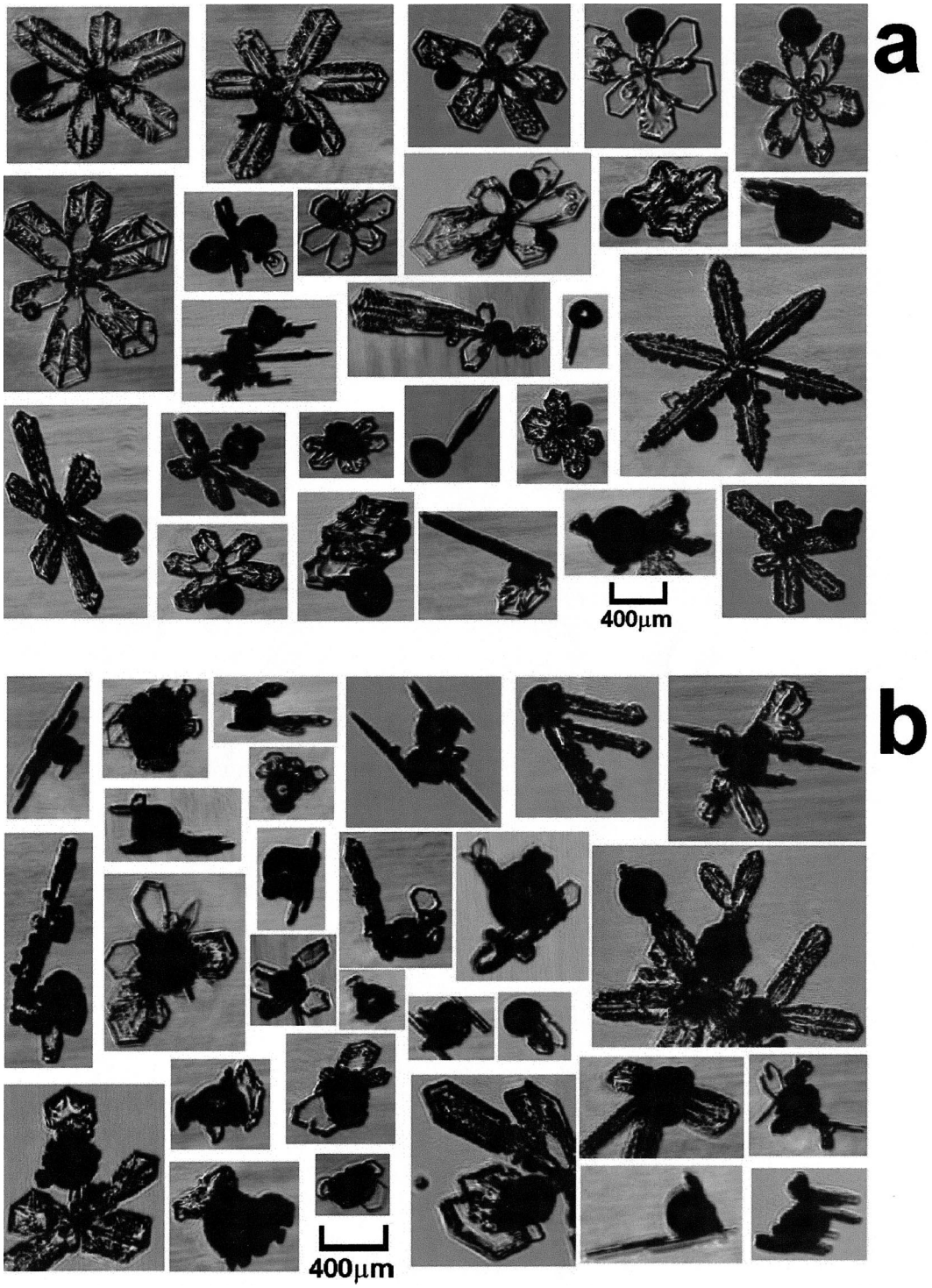

FIG. 10. Images of frozen drops measured by a CPI during a sounding between 4400 and 5600 m (Fig. 7) in a mixed-phase cloud layer: (a) drops stuck and frozen on ice particles and (b) frozen drops with subsequent growth of ice crystals.

process would likely obliterate a frozen drop, resulting in many tiny fragments, as opposed to the typically hemispherical or slightly more complete particles observed (Hallett and Isaac 2002).

The images of the ice particles in Figs. 9b and 9c are direct evidence of the existence of drop shattering in natural clouds. However, the observed concentration of shattered frozen drops is estimated as significantly smaller (less than 1%) than that of unshattered drops. Hence, it is concluded that the shattering of large drops is a rare phenomenon because it is related to the freezing drizzle formed at relatively cold temperatures (e.g., $T = -20$°C in this study). Freezing drizzle usually occurs at temperatures higher than -10°C (Cober et al. 2001) when the probability and the rate of freezing of liquid drops are lower in comparison with those at -20°C. Therefore, the probability of in situ observation of shattering at $T > -10$°C is lower than that at lower temperatures.

Figure 10a shows the images of frozen drops nucleated by collision with bigger ice particles. Most of the frozen drops have clearly a spheroidal shape without ice crystals growing out of their surface. This shape is consistent with the ground-based observation of ice crystals with cloud drops and raindrops by Kikuchi (1972) and Kikuchi and Uyeda (1979). In both cases, the frozen drops on the surface of ice crystals clearly had a spherical shape, and the ice crystals had fallen through water-saturated cloud layers.

Another group of images in Fig. 10b shows frozen drops with ice crystals growing out of certain places on their surfaces. It should be noted that the surfaces of frozen drops between ice crystals generally retain a spheroidal shape. The formation of such ice particles by aggregation is very unlikely. A possible scenario for the formation of these particles is as follows. First, the liquid drops were nucleated by collision with ice particles. Then, subsidiary ice particles start to grow from the vapor out of the frozen drops. The sizes of the secondary crystals in Fig. 10b vary from 50 to 500 μm. Because the vapor pressure in the mixed-phase layer (from 4400 to 5600 m; Fig. 7) is close to saturation over water, the growth time of the secondary crystals can be estimated from 1 to 10 min with the assumption that the temperature varies from $-12°$ to -18°C (Fig. 7c) and the rate of length growth along the a axis is 1 μm s^{-1} (e.g., Fukuta and Takahashi 1999). This time gives an estimate of the time of growth of frozen drops as spheres in natural clouds, and it is also consistent with the laboratory experiments shown in Fig. 5. The images of frozen drops with ice crystals in Fig. 10b suggest that the growth of frozen drops with $D > 100$ μm occurs differently as compared with the smaller ones described by Takahashi (1979) and Bacon et al. (2003).

6. Conclusions

Within the context of this study, the following results were obtained:

1) Spherical growth of frozen drops from vapor with diameters larger than 100 μm was observed in a thermal diffusion chamber.
2) The average growth rates of the frozen drops in still air are described well by the Maxwellian equation for the diffusional growth of ice spheroids having a density of 900 kg m^{-3}.
3) The characteristic time of spherical growth depends on temperature and supersaturation. At low supersaturation (S_i less than one-half of saturation over water), the frozen drop may keep a quasi-spherical shape during tens of minutes of growth. At higher supersaturation, individual ice crystals start to grow in different directions out of the frozen drop, eventually completely changing their shape.
4) In situ observations showed that ice crystals may grow from specific sites on the surface of a frozen drop while the remaining part of the frozen drop keeps a spheroidal shape. This observation suggests that frozen drops may be used as a tracer of freezing drizzle formed in upper-cloud layers.
5) Evidence suggestive of the shattering of large freezing drops ($D > 100$ μm) in natural clouds has been documented for the first time. CPI images collected in different clouds containing freezing drizzle suggest that shattering of large drops is a relatively rare phenomenon under these conditions.

Ice nucleation through freezing of cloud droplets plays an important role in the formation of ice in tropospheric clouds. The above results contribute to a better understanding of the evolution of ice particles during their diffusional growth.

Acknowledgments. Alexei Korolev performed this work under Contract KM175-012030/001/TOR of the Meteorological Service of Canada. The National Search and Rescue Secretariat, Transport Canada, and the Canadian Climate Action Fund provided funding for this work. Matthew Bailey and John Hallett were supported by National Science Foundation, Physical Meteorology Program Grant ATM-9900560 and NASA Grant NAG5-7973. The authors appreciate Dave Rogers (NCAR) and anonymous reviewers for useful comments.

REFERENCES

Bacon, N. J., M. B. Baker, and B. D. Swanson, 2003: Initial stages in the morphological evolution of vapor-grown ice crystals: A laboratory investigation. *Quart. J. Roy. Meteor. Soc.,* **129,** 1903–1928.

Bentley, W. A., 1907: Studies of frost and ice crystals. *Mon. Wea. Rev.,* **35,** 512–516.

Bergeron, T., 1938: Hydrometeorbeschreibungen (Definition of hydrometers). *Procès-Verbaux de la Session de Salzbourg,* Salzburg, Germany, International Meteorological Organization, No. 40, 232.

Cober, S. G., G. A. Isaac, and J. W. Strapp, 2001: Characterization of aircraft icing environments that include supercooled large drops. *J. Appl. Meteor.,* **40,** 1984–2002.

Elliott, W. P., 1971: Dimensions of thermal diffusion chambers. *J. Atmos. Sci.,* **28,** 810–810.

Fukuta, N., and T. Takahashi, 1999: The growth of atmospheric ice crystals: A summary of findings in vertical supercooled cloud tunnel studies. *J. Atmos. Sci.,* **56,** 1963–1979.

Gonda, and T. Yamazaki, 1984: Initial growth forms of snow crystals growing from frozen droplets. *J. Meteor. Soc. Japan,* **62,** 190–192.

Hallett, J., and B. J. Mason, 1958: The influence of temperature and supersaturation on the habit of ice crystals grown from the vapor. *Proc. Roy. Soc.,* **A247,** 440–453.

——, and G. A. Isaac, 2002: Aircraft icing in glaciated and mixed phase clouds. *AIAA 40th Aerospace Sciences Meeting,* Reno, NV, AIAA, Paper AIAA-2002-0677.

——, W. P. Arnott, M. P. Bailey, and J. T. Hallett, 2002: Ice crystals in cirrus. *Cirrus,* D. K. Lynch et al., Eds., Oxford University Press, 41–77.

Houghton, H. G., 1950: A preliminary qualitative analysis of precipitation mechanisms. *J. Meteor.,* **7,** 363–369.

Isaac, G. A., S. G. Cober, J. W. Strapp, A. V. Korolev, A. Tremblay, and D. L. Marcotte, 2001: Recent Canadian research on aircraft in-flight icing. *Can. Aeronaut. Space J.,* **47,** 213–221.

Jeffreys, H., 1918: Some problems of evaporation. *Philos. Mag.,* **35,** 270–280.

Johnson, D. A., and J. Hallett, 1968: Freezing and shattering of supercooled water drops. *Quart. J. Roy. Meteor. Soc.,* **94,** 468–492.

Kikuchi, K., 1972: On snow crystals with small raindrops. *J. Meteor. Soc. Japan,* **50,** 142–144.

——, and H. Uyeda, 1979: On snow crystals with small raindrops. *J. Meteor. Soc. Japan,* **57,** 273–281.

Kimura, T., and M. Kajikawa, 1984: An observation of ice pellets. *J. Meteor. Soc. Japan,* **62,** 802–808.

Knollenberg, R. G., 1981: Techniques for probing cloud microstructure. *Clouds, Their Formation, Optical Properties, and Effects,* P. V. Hobbs and A. Deepak, Eds., Academic Press, 15–91.

Kobayashi, T., 1957: Experimental researches on the snow crystal habit and growth by means of a diffusion cloud chamber. *J. Meteor. Soc. Japan,* **35,** 38–44.

Korolev, A. V., J. W. Strapp, G. A. Isaac, and A. N. Nevzorov, 1998: The Nevzorov airborne hotwire LWC–TWC probe: Principle of operation and performance characteristics. *J. Atmos. Oceanic Technol.,* **15,** 1495–1510.

Lawson, P. R., B. Baker, C. G. Schmitt, and T. Jensen, 2001: An overview of microphysical properties of Arctic clouds observed in May and June 1998 during FIRE ACE. *J. Geophys. Res.,* **106,** 14 989–15 014.

Magono, C., and C. Lee, 1966: Meteorological classification of natural snow crystals. *J. Fac. Sci. Hokkaido Univ. Ser. 7,* **2,** 321–335.

——, S. Fujita, and T. Taniguichi, 1976: Shapes of single ice crystals originated from frozen cloud drops. Preprints, *Int. Conf. on Cloud Physics,* Boulder, CO, Amer. Meteor. Soc., 103–106.

Nakaya, U., 1954: *Snow Crystals, Natural and Artificial.* Harvard University Press, 510 pp.

Pruppacher, H. R., and J. D. Klett, 1997: *Microphysics of Clouds and Precipitation.* Kluwer Academic, 954 pp.

Puzanov, V. P., and V. I. Akkuratov, 1952: About formation of some types of hailstones. *Sov. Meteor. Hydrol.,* N6, 29–33.

Takahashi, C., 1975: Deformation of frozen water drops and their frequencies. *J. Meteor. Soc. Japan,* **53,** 402–411.

——, 1976: Relation between deformation and the crystalline orientation of frozen water drops. *J. Meteor. Soc. Japan,* **54,** 448–453.

——, 1979: Formation of poly-crystalline snow crystals by riming processes. *J. Meteor. Soc. Japan,* **57,** 458–464.

Uyeda, H., and K. Kikuchi, 1978: Freezing experiments of supercooled water droplets frozen by single crystal ice. *J. Meteor. Soc. Japan,* **56,** 43–50.

Wood, S. E., M. B. Baker, and B. D. Swanson, 2002: Instrument for studies of homogeneous and heterogeneous ice nucleation in free-falling supercooled water droplets. *Rev. Sci. Instrum.,* **73,** 3988–3996.

Yamashita, A., and C. Takahashi, 1972: Initial growth process of snow crystals from frozen water drops. *Proc. Int. Cloud Physics Conf.,* London, United Kingdom, ICCP, 50–51.